

From Neutral to Anionic  $\eta^1$ -Carbon Ligands: Experimental Synthesis and Theoretical Analysis of a Rhodium–Ylidiide ComplexRemigiusz Zurawinski,<sup>†</sup> Christine Lepetit,<sup>‡,§</sup> Yves Canac,<sup>‡,§</sup> Marian Mikolajczyk,<sup>†</sup> and Remi Chauvin<sup>\*,‡,§</sup>

Center of Molecular and Macromolecular Studies, Department of Heteroorganic Chemistry, Polish Academy of Sciences, Sienkiewicza 112, 90-363 Lodz, Poland, CNRS, Laboratoire de Chimie de Coordination, 205 route de Narbonne, F-31077 Toulouse, France, and Université de Toulouse, UPS, INPT, Laboratoire de Chimie de Coordination, F-31077 Toulouse, France

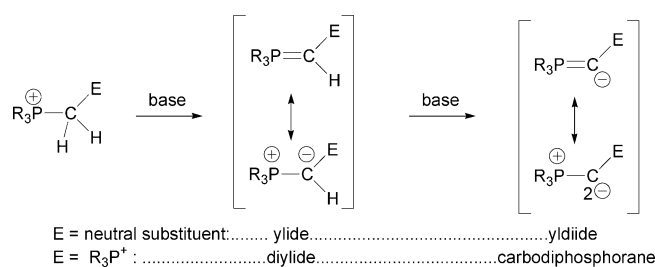
Received November 3, 2008

Deprotonation of a cationic rhodium complex of a chelating semistabilized phosphino–phosphonium sulfinyl–ylide ligand afforded the neutral complex of the corresponding ylidiide ligand. Despite the limited stability of the ylidiide complex its structure was ascertained by ESI MS and multinuclear  $^1\text{H}$ ,  $^{31}\text{P}$ ,  $^{13}\text{C}$ , and  $^{103}\text{Rh}$  NMR spectroscopy. DFT calculations were carried out at the B3PW91/6-31G\*/LANL2DZ\*(Rh) level to derive a reasonable gas-phase structure for the ylidiide complex or model thereof and gain insight into their electronic structure. ELF and AIM topological analyses were used to investigate the metal–ligand bonding and estimate the electron transfer resulting from proton abstraction. ELF weighting of the resonance forms of the anionic “free” ylidiide ligand ( $\text{Ar}_3\text{P}=\text{C}^--\text{S}(=\text{O})\text{Ar}$ ) was compared to the corresponding weighting of previously reported neutral counterparts ( $\text{X}=\text{C}=\text{Y}$ ), namely, bis- $\alpha$ -zwitterionic bisylides of phosphonium, sulfonium, or iminosulfonium moieties ( $\text{X}, \text{Y} = \text{PR}_3, \text{SR}_2, \text{S}(=\text{NMe})\text{R}_2$ ). The results suggest that the phosphonium sulfinylylidiide can be regarded as a tri- $\alpha,\beta$ -zwitteranionic bisylide ( $\text{Ar}_3\text{P}^+-\text{C}^{2-}-\text{S}^+(-\text{O}^-)p\text{-Tol}$ ).

## Introduction

On the basis of first-level thermodynamical grounds, primary alkyl phosphonium salts are expected to be significantly diacidic. On the very outset the first acidity should be indeed mainly dictated by the electrostatic effect of the geminal  $\text{P}^+$  charge in the neutral ylide, while the second acidity should be enhanced by orbital effects (also existing as secondary effects in the neutral ylide) in both the main valence bond structures of the ylidiide anion (the  $\text{sp}^2$  character of the carbon lone pair orbital in the less polar form (as compared to classical  $\text{sp}^3$  carbanions, s orbitals are indeed more “electronegative” than p orbitals)) and the forced interaction of two carbanionic lone pairs with  $\sigma^*(\text{P}-\text{C})$  empty orbitals in the  $\alpha$ -zwitteranionic form (Scheme 1).

The doubly zwitterionic nature of carbodiphosphoranes being now well established,<sup>1</sup> ylidiides can be regarded as anionic versions thereof where one of the  $\text{R}_3\text{P}^+$  substituents

**Scheme 1.** Resonance Forms of Phosphonium Ylides, Ylidiides, and Carbodiphosphoranes

is replaced by a neutral group. In spite of their thermodynamical stability phosphonium ylidiides featuring a formally dianionic carbon atom are thus anticipated to be strongly nucleophilic carbon species (Scheme 1). The resulting kinetic instability is a reason why they have been poorly studied hitherto.

To the best of our knowledge, the first mention of a phosphonium ylidiide was prompted by the observation of an unexpected reaction of pentaphenylphosphorane with an excess of *n*-butyllithium.<sup>2</sup> Later, phosphonium ylidiides were more rationally obtained by proposed lithiation of ylide

\* To whom correspondence should be addressed. Fax: (+33)5 61 55 30 03. E-mail: chauvin@lcc-toulouse.fr.

<sup>†</sup> Polish Academy of Sciences.

<sup>‡</sup> Laboratoire de Chimie de Coordination.

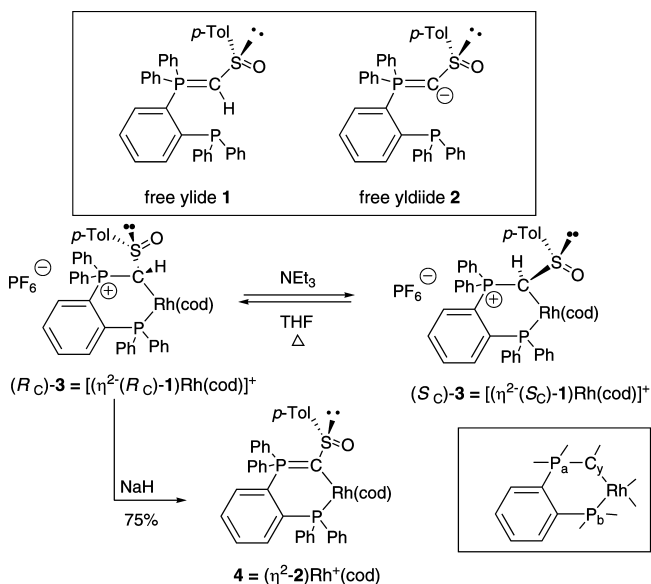
<sup>§</sup> Université de Toulouse.

precursors,<sup>3</sup> although the interpretation was revisited in a few cases.<sup>4</sup> More recently, Bertrand et al. described an original access to an  $\alpha$ -silylated lithium phosphonium ylide by 1,2-addition of *n*-butyllithium to a stable phosphanyl(silyl)carbene.<sup>5</sup> The latter ylide was submitted to a crystallographic study and shown to react with electrophiles to give the corresponding C-substituted ylides. According to Corey, as compared to ylides, yldiides exhibit an enhanced reactivity in Wittig reactions with sterically hindered ketones.<sup>3a</sup> This high reactivity was later theoretically analyzed by SCF-MO ab initio calculations.<sup>6</sup>

The nature of ylidic C–transition-metal bonds is of course more complex than that of the mostly ionic C–Li bond<sup>6</sup> due to the enhanced redox flexibility and (related) accessibility of both partly occupied (e.g., 4d) and empty (e.g., 5s, 5p) orbitals of the metal center. Such complexes have been exemplified on several occasions and formally depicted as phosphonio–carbene ligands.<sup>7</sup> The latter descriptive ambiguity actually relies on the more general analysis of ligand properties in terms of donating vs accepting character, itself refined in terms of  $\sigma/\pi$ -donation and  $\pi$ -back-donation by the Dewar–Chatt–Duncanson (DCD) model of metal–fragments near-frontier orbital interactions.<sup>8</sup> More subtle insight into the nature of the ligand–metal interaction can be gained through more sophisticated methods (energy decomposition analysis,<sup>9</sup> ELF analysis,<sup>10,11</sup> etc.).

Focusing on locally neutral  $\eta^1$ -carbon ligands we recently showed that carbon monoxide CO (and its *carbo*-mer C<sub>3</sub>O) is more  $\pi$ -accepting than ever suggested<sup>11</sup> and that a phosphonium ylide is even more donating than the NHC

**Scheme 2.** Chiral Phosphonium Ylide and Yldiides “Free” Ligands (top), Interconversion of Rhodium Complexes Thereof (middle), and Common Labeling of the Six-Membered Metacycle Atoms P<sub>a</sub>, P<sub>b</sub>, C<sub>y</sub> (bottom right)



donor paradigm.<sup>12</sup> Further deprotonation of the ylide allows for crossing the border to the realm of anionic  $\eta^1$ -carbon ligands, leading to the facing extremely donating counterparts, namely, yldiide ligands. This formal landscape is more factually explored below with the tools of both experimental synthesis and theoretical analysis.

The selected illustrative example is the yldiide deprotonated version of a previously described (sulfinylmethyl)phosphonium ylide ligand **1** (Scheme 2).<sup>13,14</sup> Considering the anticipated high reactivity of the free yldiide **2**, the rhodium complex thereof is experimentally targeted from the ylide precursor **3**, where the ylidic carbon to be deprotonated is preanchored to the rhodium center. For comparative purposes, in the basic spirit of coordination chemistry, the gas-phase properties of both the free yldiide **2** and its complex **4** will be investigated on the basis of DFT calculations and ELF topological analysis.

## Results and Discussion

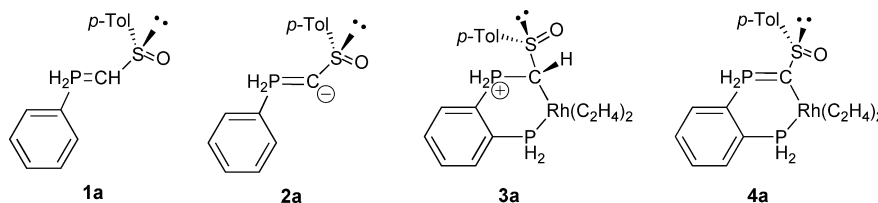
Complexes containing a resolved asymmetric ylidic carbon were previously prepared by reaction of  $[\text{Rh}(\text{cod})_2]^+$  or  $\text{PdCl}_2(\text{MeCN})_2$  with the phosphino–(sulfinylmethyl)phosphonium ylide **1**.<sup>13,14</sup> Both the (*R*<sub>C</sub>) and (*S*<sub>C</sub>) epimeric forms of the rhodium complex **3** could be obtained in inverse ratios (90:10 or 10:90) depending on the kinetic or thermodynamic conditions used in the complexation reaction.<sup>13</sup> The thermodynamic epimer **3** could also be isolated in the pure state by selective crystallization, having allowed for X-ray crystal structure determination (Table 1). It was observed that the

- (1) (a) Schmidbaur, H. *Angew. Chem., Int. Ed. Engl.* **1983**, *22*, 907. (b) Kolodiazny, O. I. *Tetrahedron* **1996**, *52*, 1855. (c) *Ylides and Imines of Phosphorus*; Johnson, A. W., Ed.; Wiley: New York, 1993. (d) Tonner, R.; Öxler, F.; Neumüller, B.; Petz, W.; Frenking, G. *Angew. Chem., Int. Ed.* **2006**, *45*, 8038. (e) Tonner, R.; Frenking, G. *Angew. Chem., Int. Ed.* **2007**, *46*, 8695. (f) Tonner, R.; Frenking, G. *Chem. Eur. J.* **2008**, *14*, 3260. (g) Tonner, R.; Frenking, G. *Chem. Eur. J.* **2008**, *14*, 3272.
- (2) Schlosser, M.; Kadibelban, T.; Steinhoff, G. *Angew. Chem., Int. Ed.* **1966**, *11*, 968.
- (3) (a) Corey, E. J.; Kang, J. *J. Am. Chem. Soc.* **1982**, *104*, 4724. (b) Corey, E. J.; Kang, J.; Kyler, K. *Tetrahedron Lett.* **1985**, *26*, 555. (c) Bestmann, H. J.; Schmidt, M. *Angew. Chem., Int. Ed.* **1987**, *26*, 79. (d) Khalil, M. I. *Main Group Met. Chem.* **1998**, *21*, 193.
- (4) (a) Schaub, B.; Jenny, T.; Schlosser, M. *Tetrahedron Lett.* **1985**, *25*, 4097. (b) Schaub, B.; Schlosser, M. *Tetrahedron Lett.* **1985**, *26*, 1623. (c) Korth, K.; Sundermeyer, J. *Tetrahedron Lett.* **2000**, *41*, 5461.
- (5) Goumri-Magnet, S.; Gornitzka, H.; Bacciredo, A.; Bertrand, G. *Angew. Chem., Int. Ed.* **1999**, *38*, 678.
- (6) McDowell, R. S.; Streitwieser, A., Jr. *J. Am. Chem. Soc.* **1984**, *106*, 4047.
- (7) See, for examples: (a) Chauvin, R. *Eur. J. Inorg. Chem.* **2000**, *577*. (b) Berno, P.; Gambarotta, S.; Kotila, S.; Erker, G. *Chem. Commun.* **1996**, 779. (c) Li, X.; Schopf, M.; Stephan, J.; Harms, K.; Sundermeyer, J. *Organometallics* **2002**, *21*, 2356. (d) Romero, P. E.; Piers, W. E.; McDonald, R. *Angew. Chem., Int. Ed.* **2004**, *43*, 6161. (e) Li, X.; Wang, A.; Sun, H.; Wang, L.; Schmidt, S.; Harms, K.; Sundermeyer, J. *Organometallics* **2007**, *26*, 3456.
- (8) (a) Dewar, M. J. S. *Bull. Soc. Chim. Fr.* **1951**, *18*, C79. (b) Chatt, J.; Duncanson, L. A. *J. Chem. Soc.* **1953**, 2929.
- (9) (a) Doerr, M.; Frenking, G. *Z. Anorg. Allg. Chem.* **2002**, *628*, 843. (b) Ziegler, T.; Rauk, A. *Theor. Chim. Acta* **1977**, *46*, 1. (c) Morokuma, K. *Acc. Chem. Res.* **1977**, *10*, 294. (d) Frenking, G. *J. Organomet. Chem.* **2001**, *635*, 9, and references therein.
- (10) Silvi, B.; Pilme, J.; Fuster, F.; Alikhani, M. E. *NATO Sci. Ser. II: Math., Phys. Chem.* **2003**, *116*, 241.
- (11) Ducéré, J. M.; Lepetit, C.; Silvi, B.; Chauvin, R. *Organometallics* **2008**, *27*, 5263.

- (12) (a) Canac, Y.; Duhayon, C.; Chauvin, R. *Angew. Chem., Int. Ed.* **2007**, *46*, 6313. (b) Canac, Y.; Lepetit, C.; Abdalilah, M.; Duhayon, C.; Chauvin, R. *J. Am. Chem. Soc.* **2008**, *130*, 8406.
- (13) Zurawinski, R.; Donnadieu, B.; Mikolajczyk, M.; Chauvin, R. *Organometallics* **2003**, *22*, 4810.
- (14) Zurawinski, R.; Donnadieu, B.; Mikolajczyk, M.; Chauvin, R. *J. Organomet. Chem.* **2004**, *689*, 380.

**Table 1.** Selected Bond Lengths (Å) and Angles (deg) Extracted from the X-ray Crystal Structure of **3** and Calculated Structure of Complexes **3** and **4** at the B3PW91/6-31G\*/LANL2DZ\*(Rh) Level

		Rh—C <sub>y</sub>	Rh—P <sub>b</sub>	C <sub>y</sub> —P <sub>a</sub>	C <sub>y</sub> —S	S=O	S—C( <i>p</i> -Tol)	Σval. ang. (C <sub>y</sub> )
exp	<b>3</b>	2.152(3)	2.2730(10)	1.764(4)	1.806(4)	1.495(3)	1.786(4)	323.8
calcd	<b>3</b>	2.150	2.339	1.801	1.845	1.517	1.806	329.0
	<b>4</b>	2.107	2.323	1.716	1.728	1.514	1.825	352.0

**Scheme 3.** Selected Models for the Free Ylide **1**, Yldiide **2**, and Rhodium Complexes Thereof **3** and **4**

thermodynamic ratio could also be obtained by heating the kinetic mixture in THF in the presence of triethylamine (Scheme 2). This was attributed to deprotonation–reprotonation equilibria of both epimers through the yldiide complex **4**.<sup>13</sup> The hypothesis remained however to be confirmed through a nonreversible deprotonation process.

**1. Synthesis and Characterization of a Rhodium Yldiide Complex (4).** It was found that treatment of **3** with a stoichiometric amount of sodium hydride in THF at  $-78$  °C affords the targeted phosphonium yldiide rhodium complex **4** in 75% yield (Scheme 2).

Complex **4** was fully characterized by multinuclear NMR spectroscopy. Its yldiide structure is first indicated by the disappearance of the ylidic <sup>1</sup>H NMR signal of **3** at  $\delta_{\text{H}} = +4.18$  ppm.<sup>13</sup> Rather surprisingly, the <sup>13</sup>C NMR chemical shifts of **4** remain very similar to those of **3**: in particular, the metallated carbon signal is almost unchanged ( $\delta_{\text{CH}}(\mathbf{3}) = +38.4$  ppm vs  $\delta_{\text{C}}(\mathbf{4}) = +41.5$  ppm). Nevertheless, the signal phase of this carbon in the J-Mod <sup>13</sup>C{<sup>1</sup>H} spectrum of **4** (ddd,  $J_{\text{CRh}} = 37.0$  Hz,  $J_{\text{CPb}} = 25.4$  Hz,  $J_{\text{CPa}} = 39.0$  Hz) clearly indicates its quaternary nature and confirms deprotonation of **3** (ddd,  $J_{\text{CRh}} = 23.3$  Hz,  $J_{\text{CPb}} = 6.4$  Hz,  $J_{\text{CPa}} = 24.8$  Hz).<sup>13</sup> The regioselectivity of the reaction at the yldiide center is also indicated by the significant shift of the phosphonium <sup>31</sup>P<sub>a</sub> signal (from +26.4 ppm in **3** to +10.4 ppm in **4**) as compared to that of the rhodium-coordinated phosphine <sup>31</sup>P<sub>b</sub> signal (+28.5 ppm in **3** and +24.3 ppm in **4**).<sup>13</sup> The corresponding coupling constants to the <sup>103</sup>Rh nucleus <sup>1</sup>J<sub>RhPb</sub> and <sup>2</sup>J<sub>RhPa</sub> vary, respectively, from 154.8 and 6.9 Hz in **3**<sup>13</sup> to 176.5 and 0 Hz in **4**.

The <sup>103</sup>Rh NMR spectrum of complex **4** was found to undergo a low field shift (+259 ppm) with respect to **3** (+170 ppm). As the yldiide ligand **2** is anticipated to be a stronger donor than the corresponding ylide ligand **1**, this observation is consistent with a general tendency found for other square-planar Rh(I) complexes of chelating dicarbon ligands: an increase of the overall basicity of the ligand (carbene–carbene < carbene–ylide < ylide–ylide) is accompanied by an increase of the  $\delta^{103}\text{Rh}$  value.<sup>12b</sup>

In contrast to the stable ylide complex **3**, complex **4** is unstable in air and decomposes even at low temperature under an inert atmosphere. The structure of the neutral complex **4** was confirmed by ESI MS and HRMS ( $m/z = 809.1643$ ) [ $\text{MH}^+$ ], giving the same value as that of the

cationic protonated precursor **3** (**3** = **4**•H<sup>+</sup>;  $m/z = 809.1636$ ),<sup>13</sup> but all attempts to grow high-quality single crystals were unsuccessful. Facing this difficulty, insights into the structure and bonding features prevailing in the yldiide complex **4** were investigated by DFT calculations.

After inspection of the performance of various DFT levels, in particular through comparison with the X-ray crystal structure of complex **3** (see Computational Details),<sup>13</sup> the structures of **3** and **4** were optimized at the B3PW91/6-31G\*/LANL2DZ\*(Rh) level (Table 1, Figure 1). Deprotonation of the ylidic carbon atom C<sub>y</sub> of **3** was thus found to induce a shortening of the three remaining adjacent bonds in the order C<sub>y</sub>–Rh ( $-0.043$  Å) < C<sub>y</sub>–P<sub>a</sub> ( $-0.085$  Å) < C<sub>y</sub>–S ( $-0.117$  Å). This suggests that the released electron density is shared between these three bonds. C<sub>y</sub> is however not perfectly planar and retains some sp<sup>3</sup> character in complex **4** (with a sum of valence angles of 352°).

The magnetic shielding tensor of **4** was also calculated at the B3PW91/6-31+G\*\*/LANL2DZ\*(Rh) level using the GIAO method. The extracted <sup>31</sup>P and <sup>13</sup>C NMR chemical shifts were compared with the experimental NMR data, and the good agreement found confirmed the interpretation discussed above (Table 2).

**2. Theoretical Analysis of the Rhodium–Yldiide Complexation. 2.1. Models of the Yldiide Complex and Corresponding “Free” Ligand.** The structure of the free yldiide ligand **2** has been investigated at the equivalent B3PW91/6-31G\* level of calculation as the one used for complex **4** (Table 3). At this level complexation of **2** to the [Rh(cod)]<sup>+</sup> moiety results in a lengthening of both the phosphonium and sulfanyl ylidic bonds ( $\Delta(\text{P}_a\text{---C}_y) = +0.054$  Å,  $\Delta(\text{S---C}_y) = +0.031$  Å) and a shortening of the adjacent ones ( $\Delta(\text{S=O}) = -0.039$  Å,  $\Delta(\text{S---Tol}) = -0.016$  Å), while the valence angle P<sub>a</sub>–C<sub>y</sub>–S is slightly decreased ( $\Delta(\text{P}_a\text{---C}_y\text{---S}) = -3.3^\circ$ ). These calculated variations are qualitatively consistent with the anticipated ones.

To obtain general insights into the nature of yldiide complexation simplified models of the free ylide **1**, yldiide **2**, and corresponding complexes **3** and **4** were envisioned. In the complex model **4a** the cyclooctadiene and PPh<sub>2</sub> moieties were thus replaced by two ethylene ligands and PH<sub>2</sub> moieties, respectively (Scheme 3). The yldiide coordination

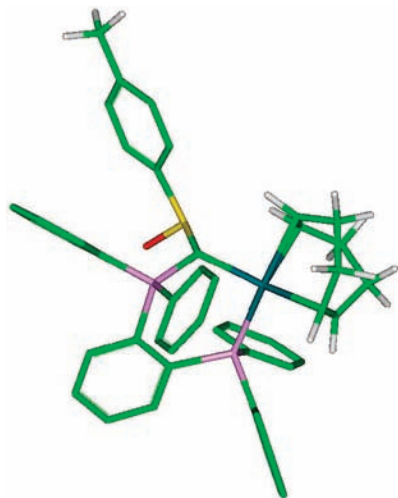


**Figure 1.** Calculated structure of complex **4** (B3PW91/6-31G\*/LANL2DZ\*(Rh)). The H atoms of the phenyl rings are omitted for clarity.

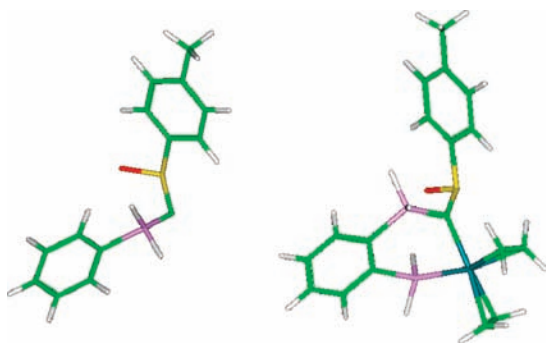


**Figure 2.** Calculated structure of the model ylide **2a** (left) B3PW91/6-31G\*) and complex thereof **4a** (right) B3PW91/6-31G\*/LANL2DZ\*(Rh)).

**Table 2.** Selected Chemical Shifts of Complex **4** (in ppm)<sup>a</sup>

	$\delta_{\text{calcd}}$	$\delta_{\text{exp}}$
<sup>31</sup> P <sub>b</sub>	28.3	24.3
<sup>31</sup> P <sub>a</sub>	12.6	10.4
<sup>13</sup> C <sub>y</sub>	58.5	41.5

<sup>a</sup> GIAO-B3PW91/6-31+G\*\*/LANL2DZ\*(Rh)// B3PW91/6-31G\*/LANL2DZ\*(Rh) level of calculation. See labeling in Scheme 2.

from **2a** to **4a** is now appraised from structural, orbital, and ELF analyses.

**2.2. Structural Analysis.** The relevance of the model **4a** is supported by the similarity between the optimized structure of the exact complex **4** and that of **4a** at the B3PW91/6-31G\*/LANL2DZ\*(Rh) level ( $\Delta/l/l < 1.8\%$ , Table 3). It is worth noting that this similarity is more satisfactory than in the protonated version, namely, between the exact ylide complex **3** and its model **3a** (see Computational Details).

In the free ligand model PhH<sub>2</sub>P=C<sup>−</sup>–S(O)*p*-Tol **2a** the PPh<sub>2</sub> moieties of **2** were deleted or replaced by a PH<sub>2</sub> moiety (Scheme 3). The relevance of this model is supported by the similarity between the calculated structures of **2** and **2a** at the B3PW91/6-31G\*\* level. Comparison of complex **4a** with the model ligand **2a** thus implicitly refers to the metallic moiety [Rh(PH<sub>2</sub>Ph)(H<sub>2</sub>C=CH<sub>2</sub>)<sub>2</sub>]<sup>+</sup> (the phenylene bridge of **4** is thus the common part in the **2a** and **4a** models).

As anticipated in the Introduction decoordination of Rh (from **4** to **2** or **4a** to **2a**) results in a shortening of the P–C

bond larger than the one of the C–S bond. This is in line with the stabilizing interaction between the  $n_{\sigma}(\text{C}_y)$  and  $\sigma^*(\text{P–Ar})$  orbitals (negative hyperconjugation) and the destabilizing interaction between the  $n_{\sigma}(\text{C}_y)$  and  $n(\text{S})$  orbitals.<sup>15</sup>

At the B3PW91/6-31+G\*\* level the ZPE-corrected proton affinities of the yl(di)idic carbon C<sub>y</sub> (ZPE-PA) of **1a** and **2a** have been estimated to be 253.9 and 372.2 kcal/mol, respectively. The huge difference (118.3 kcal/mol) is attributed to the absence of counteraction effect in the PA calculation of **2a** but also to the low PA value of **1a**, confirming its semistabilized nature. The ZPE-PA of the ylide complex **4a** vs the ylide complex **3a** is equal to 274.2 kcal/mol (for the exact complexes **4** vs **3**, PA = 296.3 kcal/mol). The latter values fall in the range of classical nonstabilized ylides<sup>16</sup> and thus show that the ylide complex **3** (or **3a**) could be also be regarded as a weakly acidic rhodomethyl–phosphonium salt while the ylide complex **4** (or **4a**) could be regarded as a rhodomethylide.

**2.3. Orbital Analysis.** The molecular orbitals (MOs) of **2a** and **4a** are shown in Figure 3. The HOMO of the free ligand **2a** corresponds to the  $\pi(\text{P}_a\text{–C}_y)$  bonding orbital that is polarized toward the C<sub>y</sub> atom as expected (Figure 3). The quasi-degenerate HOMO-1 is occupied by the second lone pair of C<sub>y</sub>, and its symmetry allows it for intervening in the coordination to rhodium in complex **4a**.

Selected MOs of complex **4a** are displayed in Figure 4. The LUMO is located, as expected, at the 16-electron Rh(I) center. As in the free ligand **2a**, the HOMO corresponds mainly to the  $\pi(\text{P}_a\text{–C}_y)$  bonding orbital that is still polarized toward the C<sub>y</sub> atom. It also exhibits a small contribution of an antibonding contribution of a rhodium d orbital. This suggests that the contribution of the phosphora–alkenyl P=C<sub>y</sub>(S)–Rh resonance form is larger than that of the phosphonio–alkylidene P<sup>+</sup>–C<sub>y</sub>(S)=Rh<sup>−</sup> form. The C<sub>y</sub>=Rh  $\pi$  bond of the latter form however occurs at lower energy as a minor component in mixing with other delocalized  $\pi$  bonds (HOMO-7 and HOMO-8). Deeper MOs contribute more significantly to the description of the underlying C<sub>y</sub>–Rh  $\sigma$  bond (HOMO-9 and HOMO-13).

**2.4. ELF Analysis.** The nature of the Rh–C<sub>y</sub> bond and electron transfer resulting from deprotonation of **3** were further investigated using electron localization function (ELF) and atoms in molecules (AIM) analyses. The chemically intuitive ELF partition of the molecular space provides basins that correspond to classical Lewis-type electronic units such as cores, bonds, and lone pairs.<sup>17</sup> Their mean populations can be interpreted in terms of weighted combinations of Lewis structures.<sup>18</sup> A statistical analysis of the ELF basin populations gives information about electron delocalization: large variance for a given basin is indicative of delocalization

(15) Pascual, S.; Asay, M.; Illa, O.; Kato, T.; Bertrand, G.; Saffon-Merceron, N.; Branchadell, V.; Baceiredo, A. *Angew. Chem., Int. Ed.* **2007**, *46*, 9078.

(16) Laavanyaa, P.; Krishnamoorthy, B. S.; Panchanatheswaran, K.; Manoharanc, M. *J. Mol. Struct. (THEOCHEM)* **2005**, *176*, 149.

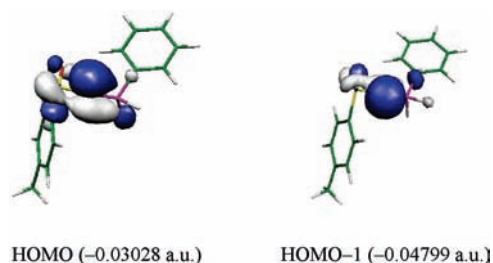
(17) (a) Becke, A. D.; Edgecombe, K. E. *J. Chem. Phys.* **1990**, *92*, 5379. (b) Silvi, B.; Savin, A. *Nature* **1994**, *371*, 683.

(18) (a) Lepetit, C.; Silvi, B.; Chauvin, R. *J. Phys. Chem. A* **2003**, *107*, 464. (b) Silvi, B. *Phys. Chem. Chem. Phys.* **2004**, *6*, 256.

**Table 3.** Selected Bond Lengths (Å) and Angles (deg) Extracted from the Calculated Structure of the Exact Ligand **2** and Complex **4** (Scheme 2) and Models Thereof **2a** and **4a** (Scheme 3)

		Rh—C <sub>y</sub>	Rh—P <sub>b</sub>	C <sub>y</sub> —P <sub>a</sub>	C <sub>y</sub> —S	S=O	S—C( <i>p</i> -Tol)	P <sub>a</sub> —C <sub>y</sub> —S ( $\Sigma$ val.) <sup>c</sup>
exact complex	<b>4</b> <sup>a</sup>	2.107	2.323	1.716	1.728	1.514	1.825	118.6 (352.0) <sup>c</sup>
exact ligand	<b>2</b> <sup>b</sup>			1.662	1.697	1.553	1.841	121.9
model complex	<b>4a</b> <sup>a</sup>	2.106	2.296	1.685	1.746	1.529	1.826	119.0 (353.9) <sup>c</sup>
model ligand	<b>2a</b> <sup>b</sup>			1.659	1.693	1.553	1.847	122.0

<sup>a</sup> B3PW91/6-31G\*/LANL2DZ\*(Rh) level. <sup>b</sup> B3PW91/6-31G\* level. <sup>c</sup> In parentheses:  $\Sigma$ val. = sum including the P<sub>a</sub>—C<sub>y</sub>—Rh and S—C<sub>y</sub>—Rh angles.

**Figure 3.** Two highest occupied MOs of **2a**. B3PW91/6-31+G\*\* level of calculation.

of its electrons, and pairwise covariance indicates the basins between which electrons are shared.<sup>18b,19</sup> Positive (respectively negative) covariances are indicative of correlated (respectively anticorrelated) basin populations. AIM charges are deduced from the populations of the corresponding atomic basins.<sup>20</sup>

The analysis was first performed on the model ylide complex **4a** and is discussed with respect to its protonated version, namely, the model chemical precursor, the ylide complex **3a**.

The scaled populations of selected ELF valence basins of **3a** and **4a** are given in Figure 5. The weights of the resonance forms fitting both these populations and the corresponding elements of the partial covariance matrix  $\langle \text{cov} \rangle$  (Supporting Information) are given in Figure 6.

From the previous description of the free ylide ligand **2a** four Lewis resonance forms may be a priori considered for describing the coordination mode in **4a** (Scheme 4).

The ELF populations suggest that the weight of forms **B** and **C** are negligible. Deprotonation of the ylide complex results in an increase of the weight of the Lewis forms with a double P=C bond from 12% in **3a** to 39% in **4a**. Concomitantly, the  $\eta^2$ -haptomeric form corresponding to a  $\pi$  bonding of the P=C bond to the Rh atom also increases from 6% in **3a** to 11% in **4a**. The C<sub>y</sub>  $\eta^1$ -bonding mode remains the major mode (94% in **3a** and 89% in **4a**). The large weight of the corresponding zwitterionic form (61%) is consistent with the nonplanarity and sizable sp<sup>3</sup> character of the ylidic carbon atom of **4a** (see section 1, Table 1).

**3. Charge Effect: Comparison of the Anionic Phosphonium Sulfinyl–Ylide **2** with Neutral Analogues.** The ylide carbon of **2** is dicoordinated to phosphonium P<sup>V</sup> and sulfinyl S<sup>IV</sup> groups. The structure of **2** thus deserved to be theoretically compared with related known compounds possessing a P<sup>V</sup>, S<sup>IV</sup>, S<sup>VI</sup>, S<sup>VI</sup>- or P<sup>V</sup>, P<sup>V</sup>-dicoordinated carbon atom: (i) the phosphonium–sulfonium bisylide **5**,<sup>15</sup> (ii) the bis-iminosulfonium bisylide **6**,<sup>21</sup> and (iii) the carbodiphos-

phorane **7** (Scheme 5).<sup>22</sup> By contrast to **2** that is anionic in nature all of three are globally neutral. The effect of the overall charge is therefore here addressed.

The neutral phosphonium–sulfonium bisylide **5** is a priori the most closely related to the anionic phosphonium sulfinyl–ylides **2** and **2a**. This has been confirmed at the B3LYP/6-31+G\*\* level of calculation (Table 4), where the calculated structures of **2a** and **5a** (a model of **5**) were found to be almost identical with very close P—C and C—S bond lengths and P—C—S valence angle. The latter, close to 120°, is wider than the corresponding angle in the X-ray crystal structures of bis-iminosulfonium bisylide **6** (116.7°) and carbodiphosporane **7** (104.8°).

By comparison to ylide **2a** (see section 2.2) the same kind of frontier orbitals have been obtained for **5** but in a reverse order.<sup>15</sup> Analogous frontier orbitals were found in the same order in a related carbodiphosporane Ph<sub>3</sub>P=C=PPh<sub>3</sub> ↔ Ph<sub>3</sub>P<sup>+</sup>—C<sup>2-</sup>—P<sup>+</sup>Ph<sub>3</sub>.<sup>1d</sup> Nevertheless, the anionic ylide **2a** and neutral analogue **5** exhibit quite similar geometry and electronic structure.

AIM and ELF analyses were performed on the optimized structures of the exact ylide **2** and known neutral analogue **5** and on the experimental crystal structures of the neutral analogues **6** and **7**. The AIM charges and scaled ELF populations of selected basins are displayed in Figure 7. It is noteworthy that the bis-iminosulfonium bisylide **6** exhibits a strongly polarized S<sup>+</sup>—N<sup>-</sup> bond (the populations of the ELF valence basins of the S—N bond and N lone pairs being equal to 2.3 and 4.2, respectively). It is however weaker than the polarization of the S<sup>+</sup>—O<sup>-</sup> bond in the sulfinyl ylide **2**, which implies a purely ionic S<sup>2+</sup>...O<sup>2-</sup> contribution (the populations of the ELF valence basins of the S—O bond and O lone pairs being equal to 1.3 and 6.6, respectively).

At first glance the AIM charges in the structures **2**, **5**, **6**, and **7** seem to be erratic. It is however noticeable that the AIM charge of the central C<sub>y</sub> atom can be accurately expressed as a sum of independent parameters for the charge transfer from either a P<sup>V</sup> or a S<sup>V ± I</sup> substituent: in any of the four X=C=Y structures,  $Q_{\text{AIM}}(\text{C}_y) = Q(\text{X}) + Q(\text{Y})$ , where  $Q(\text{P}^{\text{V}}) = -1.15$  and  $Q(\text{S}^{\text{V} \pm \text{I}}) = -0.35$ . In particular, the C<sub>y</sub> AIM charge of **2** and **5** bearing the same substituent set (X = P<sup>V</sup>, Y = S<sup>V ± I</sup>) is exactly the same (-1.5). The AIM charge of the central carbon is thus strongly correlated to the nature of the adjacent heteroatoms. More generally, the AIM and ELF similarity between **2** and **5** is striking.

The weights of the resonance forms fitting the above ELF valence basin populations are given in Figure 8. On the basis of the populations, the weight of the X=C=Y forms have been

(19) Savin, A.; Silvi, B.; Colonna, F. *Can. J. Chem.* **1996**, *74*, 1088.

(20) Bader, R. F. W. *Atoms In Molecules*; Clarendon Press: Oxford, 1990.

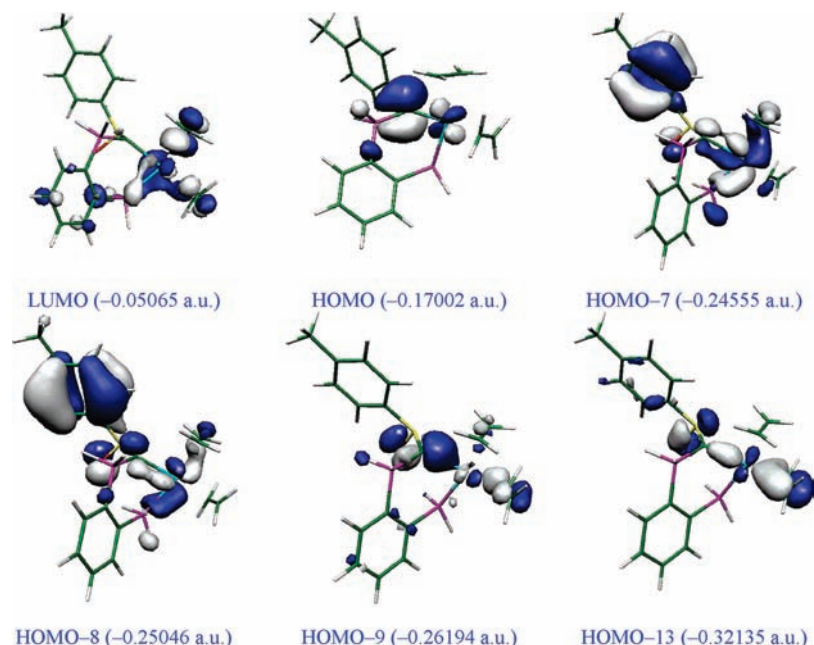


**Figure 4.** Selected MOs of **4a**. B3PW91/6-31G\*/LANL2DZ\*(Rh) level of calculation. The corresponding eigenvalues are indicated in parentheses (in atomic units).

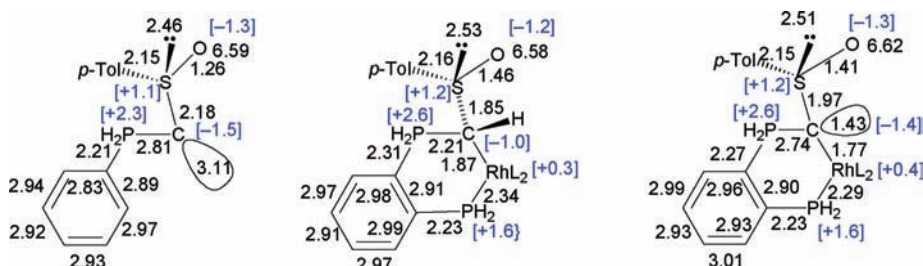


**Figure 5.** ELF valence basins populations of **2a** (left), **3a** (middle), and **4a** (right). AIM charges in square brackets. B3PW91/6-31G\*/DGDZVP(Rh) level of calculation. Geometry of **2a** calculated at the B3PW91/6-31G\* level, and those of **3a** and **4a** calculated at the B3PW91/6-31G\*/LANL2DZ(Rh) level. The monosynaptic valence basin  $V(C_y)$  is explicitly indicated by a foil (those at O atoms are implicit).

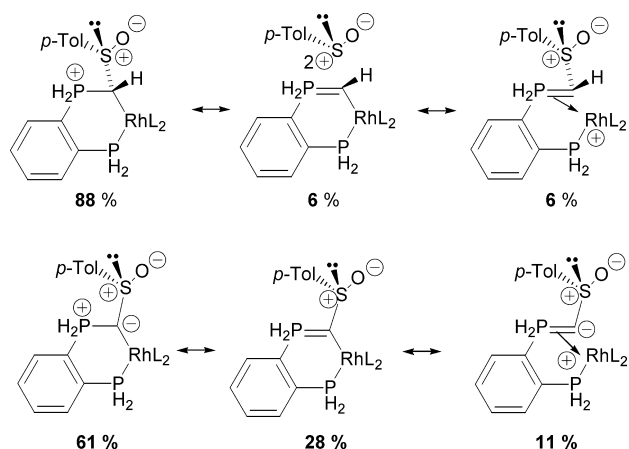
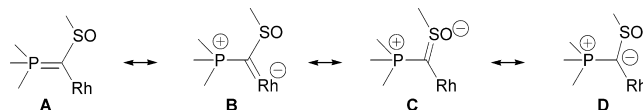


**Figure 6.** More representative Lewis structures of **3a** (top) and **4a** (bottom) in agreement with the ELF valence basins populations of Figure 5.

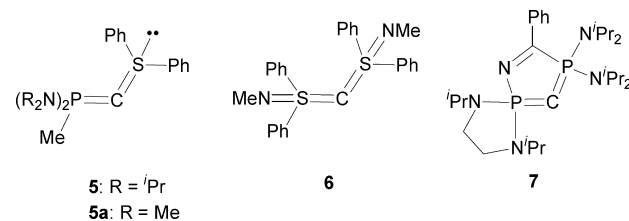
been set to zero. Most of the components of the partial covariance matrix  $\langle \text{cov} \rangle$  are compatible with the above description.

Over the whole series the Lewis form featuring a dianionic  $C_y$  is always the major one. The symmetrical bis-iminosulfonium bisylide **6** possesses the largest weight of this form (60%), while the carbodiphosphorane **7** exhibits the lowest one (35%). The phosphonium sulfanyl-yldiide **2** and phosphonium-sulfonium bisylide **5** exhibit intermediate values

**Scheme 4.** Possible Resonance Forms Describing the Coordination of the Yldiide Ligands **2** or **2a** to Rhodium



**Scheme 5.** Schematic Apolar Representations of Known Neutral Analogues or Models Thereof of the Phosphonium Sulfinyl-Yldiide **2**



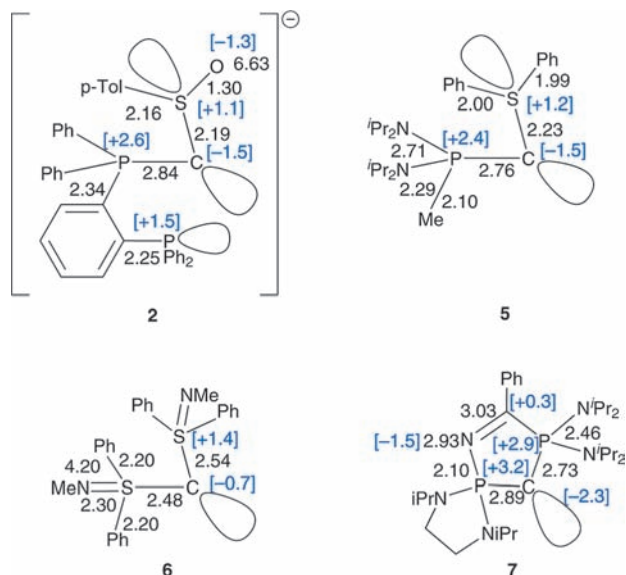
of the dianionic  $C_y$  weight that are noticeably very close (46% for **2** and 42% for **5**). Whatever the criterion (AIM charge or weight of the dianionic  $C_y$  Lewis structure extracted from ELF analysis), the global charge is found to exert a weak influence on the “nucleophilic” character and thus the “precoordinating” ability of the  $C_y$  carbon of **2** and **5**.

It is also worth noting that in both **2** and **5** the weight of the Lewis form featuring a double  $P=C$  bond (31–37%) is

**Table 4.** Selected Bond Lengths (Å) and Angles (deg) Extracted from the Calculated Structure of the Anionic Ylide **2a** and the Neutral Phosphonium–Sulfonium Bisylyde Model **5a**<sup>15a</sup>

	P <sub>a</sub> –C <sub>y</sub>	C <sub>y</sub> –S	S–O	S–C(Tol)	P <sub>a</sub> –C <sub>y</sub> –S
<b>2a</b>	1.676	1.710	1.568	1.871	120.0
<b>5a</b>	1.675	1.682			119.4
<b>5</b>	1.675	1.669			117.7

<sup>a</sup> B3LYP/6-31+G\*\* level of calculation (see labeling in Scheme 2).

**Figure 7.** Comparison of scaled populations of selected ELF valence basins of **2**, **5**, **6**, and **7**. Monosynaptic valence basins of C<sub>y</sub>, S, and P<sub>b</sub> atoms are explicitly indicated by a foil (those at O or N atoms are implicit). AIM charges are given in square brackets. B3PW91/6-31G\* level of calculation. Geometries used: B3PW91/6-31G\* for **2**, B3LYP/6-31+G\*\* for **5**, and experimental crystal structures for **6** and **7**.**Table 5.** Experimental and Calculated Structure of Complex **3**: Bond Lengths (Å)

		Rh–C <sub>y</sub>	Rh–P <sub>b</sub>	C <sub>y</sub> –P <sub>a</sub>	C <sub>y</sub> –S	S=O	S–C ( <i>p</i> -Tol)
	X-ray data	2.152	2.273	1.764	1.806	1.495	1.786
exact	B3PW91 <sup>a</sup>	2.150	2.339	1.801	1.845	1.517	1.806
complex <b>3</b>	PBE <sup>a</sup>	2.148	2.337	1.809	1.871	1.535	1.825
	B3LYP <sup>a</sup>	2.171	2.358	1.809	1.864	1.523	1.817
model <b>3a</b>	B3PW91 <sup>a</sup>	2.106	2.295	1.786	1.852	1.516	1.802
	B3PW91 <sup>b</sup>	2.109	2.297	1.785	1.852	1.516	1.802
model <b>3b</b>	B3PW91 <sup>a</sup>	2.124	2.306	1.789	1.851	1.515	1.804
	B3PW91 <sup>b</sup>	2.127	2.307	1.788	1.850	1.515	1.804

<sup>a</sup> 6-31G\*/LANL2DZ\*(Rh) basis set. <sup>b</sup> 6-31G\*/LANL2DZ(Rh) basis set.

**Table 6.** Selected Bond Lengths (Å) and Angles (deg) Extracted from the Calculated Structure of Complex **4** and Model Thereof **4a** and **4b**<sup>a</sup>

	Rh–C <sub>y</sub>	Rh–P <sub>b</sub>	C <sub>y</sub> –P <sub>a</sub>	C <sub>y</sub> –S	S=O	S–C( <i>p</i> -Tol)	Σval. ang. (C <sub>y</sub> )
<b>4a</b>	2.106	2.296	1.685	1.746	1.529	1.826	353.9
<b>4b</b>	2.101	2.299	1.697	1.735	1.533	1.827	355.1
<b>4</b>	2.107	2.323	1.716	1.728	1.514	1.825	352.0

<sup>a</sup> B3PW91/6-31G\*/LANL2DZ\*(Rh) level of calculation.

larger than the one featuring a double C=S bond (5–6%). This is in agreement with the indirect structural criterion of the relative C–P and C–S bond lengths (Table 4).

The noticeable ELF and AIM analogy between **2** and **5** is explained by the strong polarization of the S–O bond of **2** (the anionic charge is thus repelled on the sulfinyl oxygen atom). In spite of their difference in overall charge,

the resemblance of their Lewis description is thus consistent with the similarity of their geometry and electronic structure.

One has however to remember that the weight of ionic structures is expected to be both intrinsically and indirectly slightly overestimated in particular because the ELF function is here obtained from a DFT monodeterminantal evaluation of the electron density.<sup>18b</sup>

## Conclusion

“Ylides complexes” were thus shown to deserve their name in the chemical sense. The rhodium representative **4** was indeed obtained by deprotonation of an ylide complex precursor **3**. Ylides belong to the class of anionic  $\eta^1$ -carbon ligands with a formal sp<sup>2</sup> hybridization state of the coordinated carbon atom. The bonding properties of this kind of ligands have been investigated at the DFT level using structural, orbital, and electronic density criteria. Detailed ELF analysis allowed assigning two main representative resonance forms for the static description of both the free ligand and rhodium complexes thereof. The strong analytical analogy with known neutral version shows that the overall charge, making the free ylide ligands unstable, exerts a very weak influence on the bonding properties. Whereas nonstabilized ylides were mainly described as phosphonio–alkenylidene ligands at ruthenium(II) centers (P<sup>+</sup>–CH=[Ru]<sup>–</sup>),<sup>7d</sup> the sulfinyl substituent of **2** is certainly determining in assigning the strong phosphora–alkenyl character of the ligand at the rhodium(I) center (P=C(SO-*p*Tol)–[Rh]). Nonetheless, the specific catalytic properties induced by the former ligand type are inviting investigations of possible applications of the latter ligand type, after further stabilization by suitable substituents, in rhodium-catalyzed processes.<sup>23</sup>

## Experimental Section

**General Remarks.** THF was dried and distilled over sodium/benzophenone and dichloromethane over P<sub>2</sub>O<sub>5</sub>. All other reagents were used as commercially available. All reactions were carried out under an argon atmosphere using Schlenk and vacuum line techniques. The following analytical instruments were used. <sup>1</sup>H, <sup>13</sup>C, <sup>31</sup>P, and <sup>103</sup>Rh NMR: Bruker ARX 250, DPX 300, or AV 500. Mass spectrometry: Quadrupolar Nermag R10-10H. NMR chemical shifts  $\delta$  are in ppm with positive values to high frequency relative to the tetramethylsilane reference for <sup>1</sup>H and <sup>13</sup>C and to H<sub>3</sub>PO<sub>4</sub> for <sup>31</sup>P. <sup>103</sup>Rh chemical shifts are given to high frequency of  $\Xi$ (<sup>103</sup>Rh) = 3.16 MHz; coupling constants *J* are in Hz.

**4.** To a stirred solution of sodium hydride (7.3 mg, 0.304 mmol) in THF (2 mL) at –78 °C was added a solution of Rh complex **3** (0.29 g, 0.304 mmol) in THF (3 mL). The suspension was warmed to 0 °C and stirred for 1 h. After evaporation of the solvent, CH<sub>2</sub>Cl<sub>2</sub> (5 mL) was added and the suspension was filtered. Evaporation of the solvent under vacuum afforded **4** as a brown oil (0.18 g, 75%).

- Fujii, T.; Ikeda, T.; Mikami, T.; Suzuki, T.; Yoshimura, T. *Angew. Chem., Int. Ed.* **2002**, *41*, 2576.
- Marrot, S.; Kato, T.; Gornitzka, H.; Bacciredo, A. *Angew. Chem., Int. Ed.* **2006**, *45*, 2598.
- (a) Wenzel, A. G.; Grubbs, R. H. *J. Am. Chem. Soc.* **2006**, *128*, 16048. (b) Getty, K.; Delgado-Jaime, M. U.; Kennepohl, P. *J. Am. Chem. Soc.* **2007**, *129*, 15774. (c) van der Eide, E. F.; Romero, P. E.; Piers, W. E. *J. Am. Chem. Soc.* **2008**, *130*, 4485.

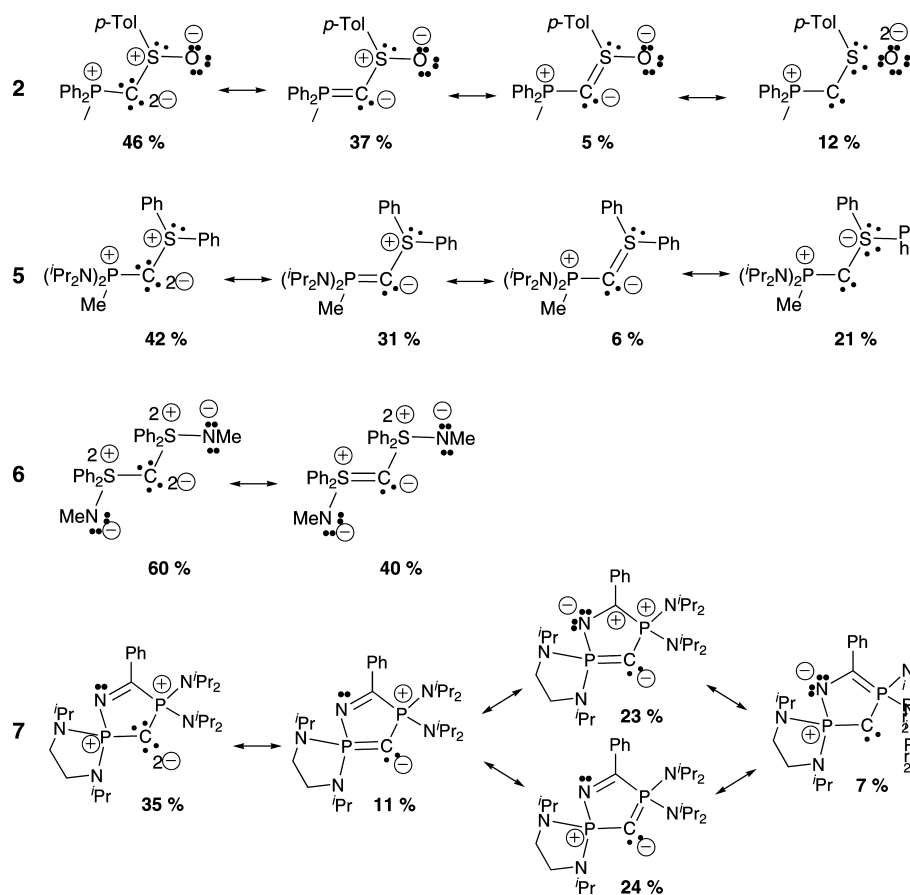
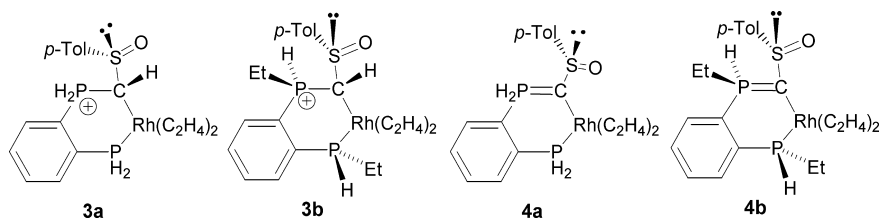


**Figure 8.** Weighted Lewis structures of **2**, **5**, **6**, and **7**, in agreement with the ELF valence basins populations and covariances.

**Scheme 6.** Model Rhodium Complexes for the Exact Experimental Complexes **3** and **4**



$^{31}\text{P}\{^1\text{H}\}$  NMR (THF- $d_8$ , 5 °C):  $\delta = +24.3$  (dd,  $J_{\text{PbRh}} = 176.5$  Hz,  $J_{\text{PbPa}} = 42.5$  Hz, Pb),  $+10.4$  (d,  $J_{\text{PaPb}} = 42.5$  Hz, Pa).  $^1\text{H}$  NMR (THF- $d_8$ , 5 °C):  $\delta = 6.91$ – $8.22$  (m, 26H,  $\text{CH}_{\text{ar}}$ ),  $6.72$  (d,  $J_{\text{HH}} = 7.6$  Hz, 2H,  $\text{CH}_{\text{ar}}$ ),  $6.68$  (brs, 2H,  $\text{CH}_{\text{cod}}$ ),  $2.95$  (brs, 1H,  $\text{CH}_{\text{cod}}$ ),  $2.81$  (brs, 1H,  $\text{CH}_{\text{cod}}$ ),  $2.31$  (s, 3H,  $\text{CH}_3$ ),  $1.55$ – $2.10$  (m, 7H,  $\text{CH}_{2\text{cod}}$ ),  $1.30$ – $1.45$  (m, 1H,  $\text{CH}_{2\text{cod}}$ ).  $^{13}\text{C}$  NMR (THF- $d_8$ , 5 °C):  $\delta = 150.80$  (d,  $J_{\text{CPa}} = 33.4$  Hz,  $\text{S}(\text{O})\text{C}_{\text{ar}}$ ),  $139.07$  (dd,  $J_{\text{CPa}} = 95.9$  Hz,  $J_{\text{CPb}} = 17.8$  Hz,  $\text{C}_{\text{ar}}$ ),  $138.21$  (d,  $J_{\text{CPa}} = 7.0$  Hz,  $\text{CH}_{\text{ar}}$ ),  $137.57$  (d,  $J_{\text{CPa}} = 88.4$  Hz,  $\text{C}_{\text{ar}}$ ),  $135.63$  (dd,  $J_{\text{CPb}} = 37.2$  Hz,  $J_{\text{CPa}} = 6.4$  Hz,  $\text{C}_{\text{ar}}$ ),  $135.23$  (s,  $\text{C}_{\text{ar}}\text{CH}_3$ ),  $134.66$  (d,  $J_{\text{CPb}} = 38.8$  Hz,  $\text{C}_{\text{ar}}$ ),  $134.33$  (d,  $J_{\text{CPa}} = 7.6$  Hz,  $\text{CH}_{\text{ar}}$ ),  $134.13$  (m,  $\text{CH}_{\text{ar}}$ ),  $133.86$  (d,  $J_{\text{CPb}} = 11.5$  Hz,  $\text{CH}_{\text{ar}}$ ),  $133.46$  (d,  $J_{\text{CPb}} = 45.4$  Hz,  $\text{C}_{\text{ar}}$ ),  $132.73$  (d,  $J_{\text{CPa}} = 9.9$  Hz,  $\text{CH}_{\text{ar}}$ ),  $132.37$  (d,  $J_{\text{CPb}} = 10.3$  Hz,  $\text{CH}_{\text{ar}}$ ),  $131.00$  (d,  $J_{\text{CPb}} = 4.0$  Hz,  $\text{CH}_{\text{ar}}$ ),  $130.68$  (s,  $\text{CH}_{\text{ar}}$ ),  $130.32$  (s,  $\text{CH}_{\text{ar}}$ ),  $129.77$  (s,  $\text{CH}_{\text{ar}}$ ),  $129.22$  (d,  $J_{\text{CPa}} = 10.5$  Hz,  $\text{CH}_{\text{ar}}$ ),  $129.06$  (s,  $\text{CH}_{\text{ar}}$ ),  $128.65$  (d,  $J_{\text{CPb}} = 10.0$  Hz,  $\text{CH}_{\text{ar}}$ ),  $128.55$  (d,  $J_{\text{CPa}} = 10.0$  Hz,  $\text{CH}_{\text{ar}}$ ),  $128.44$  (d,  $J_{\text{CPb}} = 8.4$  Hz,  $\text{CH}_{\text{ar}}$ ),  $127.85$  (d,  $J_{\text{CPa}} = 10.5$  Hz,  $\text{CH}_{\text{ar}}$ ),  $127.74$  (s, 2  $\text{CH}_{\text{ar}}$ ),  $127.58$  (d,  $J_{\text{CPb}} = 9.0$  Hz,  $\text{CH}_{\text{ar}}$ ),  $126.34$  (s,  $\text{CH}_{\text{ar}}$ ),  $102.83$  (dd,  $J_{\text{CRh}} = 8.3$  Hz,  $J_{\text{CPb}} = 8.3$  Hz,  $\text{CH}_{\text{cod}}$ ),  $99.26$  (brs,  $\text{CH}_{\text{cod}}$ ),  $79.95$  (brs,  $\text{CH}_{\text{cod}}$ ),  $76.21$  (d,  $J_{\text{CRh}} = 7.9$  Hz,  $\text{CH}_{\text{cod}}$ ),  $41.5$  (br ddd,  $J_{\text{CRh}} = 37.0$  Hz,  $J_{\text{CPb}} = 25.4$  Hz,  $J_{\text{CPa}} = 39.0$  Hz,  $\text{PCRh}$ ),  $31.36$  (s,  $\text{CH}_{2\text{cod}}$ ),  $31.21$  (s,  $\text{CH}_{2\text{cod}}$ ),  $28.78$  (s,  $\text{CH}_{2\text{cod}}$ ),  $28.43$  (s,  $\text{CH}_{2\text{cod}}$ ),  $20.31$  (s,

$\text{CH}_3$ ).  $^{103}\text{Rh}$  NMR ( $\text{CDCl}_3$ , 25 °C):  $\delta = +259$ . MS( $\text{ES}^+$ ):  $m/z$ : 809 [ $\text{MH}^+$ ]. HRMS ( $\text{ES}^+$ ) calcd for  $\text{C}_{46}\text{H}_{44}\text{SOP}_2\text{Rh}$ , 809.1677; found, 809.1643.

### Computational Details

**General Remarks.** Geometries were fully optimized at various DFT levels using Gaussian03.<sup>24</sup> The LANL2DZ\*(Rh) basis set includes f-polarization functions derived by Ehlers et al. for Rh that have been added to the LANL2DZ(Rh) basis set.<sup>25</sup> Vibrational analysis was performed at the same level as the geometry optimization. The magnetic shielding tensor was calculated at the B3PW91/6-31+G\*\*/LANL2DZ\*(Rh) level using the GIAO (gauge-independent atomic orbital) method implemented in Gaussian 03.<sup>24</sup> The  $^{31}\text{P}$  NMR and  $^{13}\text{C}$  NMR chemical shifts were estimated with respect to the usual  $\text{H}_3\text{PO}_4$  and TMS ( $\text{SiMe}_4$ ) references. Frontier orbitals contours were drawn with the Molekel visualization package.<sup>26</sup> AIM and ELF analyses were performed with the TopMoD package.<sup>27</sup>

**Selection of the Calculation Level for Rhodium Complexes.** The calculation level was first investigated on the ylide complex **3** for which an X-ray crystal structure is available.<sup>13</sup> Various functionals were examined (Tables 1 and 5). With the 6-31G\*/LANL2DZ\*(Rh)



basis set all attempted functionals afforded satisfactory results and in particular good estimates of the Rh–C<sub>y</sub> bond length. Despite the uncertainty of the esd values it is however noteworthy that the Rh–P<sub>b</sub> bond is overestimated by 0.9 Å with B3LYP and 0.07 Å with B3PW91. The same pitfall of hybrid functionals was observed by Zhao et al. for BINAP complexes of ruthenium, whereas GGA (PBE or PW91) functionals were shown to perform better.<sup>28</sup> This is however not the case here (Table 5), and the B3PW91/6-31G\*/LANL2DZ\*(Rh) level of calculation is selected hereafter as the best compromise.

Model complexes **3a,b** were thus considered (Scheme 6), where the cyclooctadiene ligand is replaced by two ethylene ligands whereas the phenyl substituents of the phosphorus atoms are substituted either by two H atoms (**a**) or by one H atom and one ethyl group (**b**). This latter case allows for a better description of the electronic and steric effect of the P substituents. The Tolman electronic parameter of PHEt (10.1°) is indeed closer to the one of PPh<sub>2</sub> (8.6°) than that of PPh<sub>2</sub> (16.6°).<sup>29</sup> However, in contrast to complex **3** the P<sub>b</sub> atom of **3b** is a stereogenic center.

At the B3PW91/6-31G\*/LANL2DZ(Rh) level the calculated structures of model complexes **3a** and **3b** are in quite good agreement with the experimental structure of **3** but exhibit shorter Rh–C<sub>y</sub> bonds than in **3**. The model **3b** however performs better than **3a**, suggesting that the bond shortening can be ascribed to an imperfect modeling of the electronic effects of the exocyclic P substituents. The artificial P stereogenicity in **3b** also induces distortions of the metallacycle that are not present in the experimental structure. It is finally noteworthy that substitution of the cyclooctadiene ligand by two ethylene molecules is satisfactory. The P–Rh–C<sub>y</sub> angle of the calculated structure **3a** (89.9°) is indeed in good agreement with that of the experimental structure (92.3°) and the calculated structure of **3** (90.7°).

The structures of the ylidiide complex **4** and models thereof **4a** and **4b** were also calculated (Scheme 6 and Table 6), and the optimized geometries were found to be quite similar. In all cases, proton abstraction from the ylidic carbon atom of **3**, **3a**, or **3b** results in a shortening of the remaining adjacent bonds (see Discussion section 2.1).

**Acknowledgment.** This work was performed with the support of the Laboratoire Européen Associé (LEA) financed by the CNRS in France, and by the Ministry of Science and Higher Education in Poland. The authors also thank CALMIP (Calcul intensif en Midi-Pyrénées, Toulouse, France), IDRIS (Institut du Développement et des Ressources en Informatique Scientifique, Orsay, France), and CINES (Centre Informatique de l'Enseignement Supérieur, Montpellier, France) for computing facilities.

**Supporting Information Available:** ELF truncated population vector  $\langle N \rangle$  and covariance matrix  $\langle \text{cov} \rangle$  of ligands **2** and **5–7** and complexes **3a** and **4a**; Cartesian coordinates, level of calculation, total energies in atomic units of structures of structures **2–5** and their models. This material is available free of charge via the Internet at <http://pubs.acs.org>.

IC802104F

- (24) Frisch, M. J.; Trucks, G. W.; Schlegel, H. B.; Scuseria, G. E.; Robb, M. A.; Cheeseman, J. R.; Montgomery, Jr., J. A.; Vreven, T.; Kudin, K. N.; Burant, J. C.; Millam, J. M.; Iyengar, S. S.; Tomasi, J.; Barone, V.; Mennucci, B.; Cossi, M.; Scalmani, G.; Rega, N.; Petersson, G. A.; Nakatsuji, H.; Hada, M.; Ehara, M.; Toyota, K.; Fukuda, R.; Hasegawa, J.; Ishida, M.; Nakajima, T.; Honda, Y.; Kitao, O.; Nakai, H.; Klene, M.; Li, X.; Knox, J. E.; Hratchian, H. P.; Cross, J. B.; Adamo, C.; Jaramillo, J.; Gomperts, R.; Stratmann, R. E.; Yazyev, O.; Austin, A. J.; Cammi, R.; Pomelli, C.; Ochterski, J. W.; Ayala, P. Y.; Morokuma, K.; Voth, G. A.; Salvador, P.; Dannenberg, J. J.; Zakrzewski, V. G.; Dapprich, S.; Daniels, A. D.; Strain, M. C.; Farkas, O.; Malick, D. K.; Rabuck, A. D.; Raghavachari, K.; Foresman, J. B.; Ortiz, J. V.; Cui, Q.; Baboul, A. G.; Clifford, S.; Cioslowski, J.; Stefanov, B. B.; Liu, G.; Liashenko, A.; Piskorz, P.; Komaromi, I.; Martin, R. L.; Fox, D. J.; Keith, T.; Al-Laham, M. A.; Peng, C. Y.; Nanayakkara, A.; Challacombe, M.; Gill, P. M. W.; Johnson, B. W.; Wong, W.; Gonzalez, C. and Pople, J. A., *Gaussian 03*, Revision B.05; Gaussian, Inc.: Pittsburgh, PA, 2003.
- (25) Ehlers, A. W.; Böhme, M.; Dapprich, S.; Gobbi, A.; Höllwarth, A.; Jonas, V.; Köhler, K. F.; Stegmann, R.; Veldkamp, A.; Frenking, G. *Chem. Phys. Lett.* **1993**, *208*, 111.
- (26) Portmannand, S.; Flükiger, P. F.; Lüthi, H. P.; Weber, J. *Molekel 4.3*; University of Geneva and Swiss Center for Scientific Computing: Manno, Switzerland, 2002; [www.cscs.ch/molekel/](http://www.cscs.ch/molekel/).
- (27) Noury, S.; Krokidis, X.; Fuster, F.; Silvi, B. *Comput. Chem.* **1999**, *23*, 597.
- (28) Zhao, Y. X.; Wang, S. G. *Chin. Chem. Lett.* **2005**, *16*, 1555.
- (29) Tolman, C. A. *J. Am. Chem. Soc.* **1970**, *92*, 2953.